

# Quantitation of Protein Adducts of Aristolochic Acid I by Liquid Chromatography–Tandem Mass Spectrometry: A Novel Method for Biomonitoring Aristolochic Acid Exposure

Chi-Kong Chan, Kwan-Kit Jason Chan, Ning Liu,\* and Wan Chan\*



Cite This: *Chem. Res. Toxicol.* 2021, 34, 144–153



Read Online

ACCESS |



Metrics & More

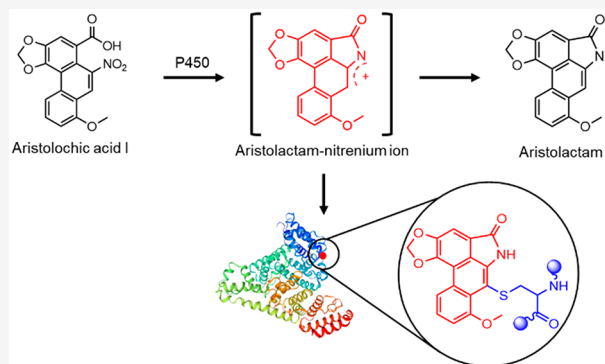


Article Recommendations



Supporting Information

**ABSTRACT:** Emerging evidence suggests that chronic exposure to aristolochic acids (AAs) is one of the etiological pathways leading to chronic kidney disease (CKD). Due to the traditional practice of herbal medicine and AA-containing plants being used extensively as medicinal herbs, over 100 million East Asians are estimated to be at risk of AA poisoning. Given that the chronic nephrotoxicity of AAs only manifests itself after decades of exposure, early diagnosis of AA exposure could allow for timely intervention and disease risk reduction. However, an early detection method is not yet available, and diagnosis can only be established at the end stage of CKD. The goal of this study was to develop a highly sensitive and selective method to quantitate protein adducts of aristolochic acid I (AAI) as a biomarker of AA exposure. The method entails the release of protein-bound aristolactam I (ALI) by heat-assisted alkaline hydrolysis, extraction of ALI, addition of internal standard, and quantitation by liquid chromatography–tandem mass spectrometric analysis. Accuracy and precision of the method were critically evaluated using a synthetic ALI-containing glutathione adduct. The validated method was subsequently used to detect dose-dependent formation of ALI–protein adducts in human serum albumin exposed to AAI and in proteins isolated from the tissues and sera of AAI-exposed rats. Our time-dependent study showed that ALI–protein adducts remained detectable in rats even at 28 days postdosing. It is anticipated that the developed method will fill the technical gap in diagnosing AA intoxication and facilitate the biomonitoring of human exposures to AAs.



## INTRODUCTION

Latest epidemiological studies have shown that chronic kidney disease (CKD) is surprisingly affecting around 10% of the global population,<sup>1</sup> especially in developing countries,<sup>2–4</sup> causing tremendous suffering and taking away millions of lives annually.<sup>3</sup> Being a multifactorial disease, CKD could be caused by diabetes, high blood pressure, exposure to toxicants, and many other factors.<sup>5,6</sup> The large population of CKD patients imposes a heavy burden on public healthcare systems;<sup>7</sup> thus, the identification of the etiological agents of CKD will provide crucial information for regulatory agencies to implement policies on reducing human exposure risks and assist in devising methods for early detection of such risks.

Emerging evidence suggests that chronic exposure to aristolochic acids (AAs, Figure 1), a family of highly potent nephrotoxins produced naturally in *Aristolochia* and *Asarum* plants, is one of the major causes of CKD.<sup>8–12</sup> Due to the traditional practice of herbal medicine and the extensive use of AA-containing plants in many traditional herbal medicine preparations,<sup>8,13</sup> it is estimated that over 100 million people in East Asia are at risk of AA poisoning, which could eventually lead to the development of CKD and urothelial cancers.<sup>13</sup>

Furthermore, residents of rural farming villages in the Balkan Peninsula are also suffering from a unique and slowly progressive form of renal disease, known as the Balkan endemic nephropathy (BEN), caused by the dietary intake of AA-contaminated food and underground water.<sup>8,14–20</sup>

Being able to identify the population at high risk of developing AA-associated nephropathy will allow for a timely intervention and an improved chance of recovery. Previous studies confirmed AA intoxication by detecting aristolactam (AL)–DNA adducts in the renal cortex of BEN patients.<sup>14,21–23</sup> However, that analysis involves the use of DNA samples isolated from kidney tissues obtained in a biopsy, which is an invasive sampling procedure that poses risks of bleeding and infection.<sup>24</sup> Thus, this analysis normally uses surgical specimens collected during kidney transplantation

Received: October 17, 2020

Published: January 7, 2021



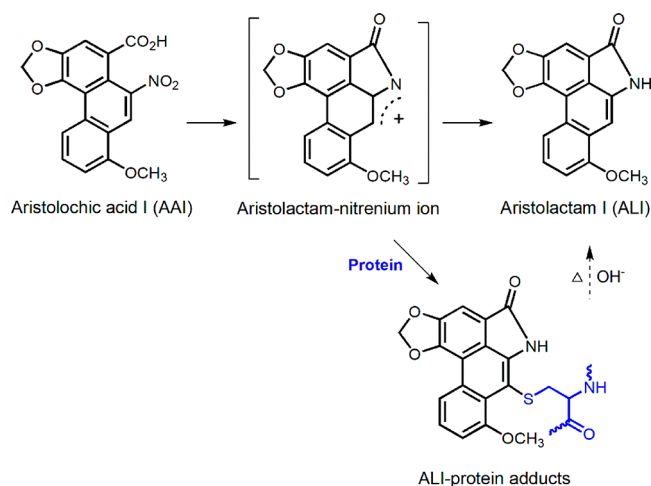


**Figure 1.** Metabolic activation and protein adduct formation of aristolochic acid I.

in patients suffering from end-stage kidney failure.<sup>25</sup> To the best of our knowledge, biomarkers and methods that would allow for an early diagnosis of AA poisoning are currently not yet available in the literature.

The present study focuses on the more accessible blood proteins as the target molecules to use as biomarkers for AA exposure. There are three main reasons for us to target proteins in this study. First, proteins are the most abundant macromolecules in living systems, making up to half of the dry weight of cells (DNA ~3%).<sup>26</sup> Thus, cellular proteins are likely to receive more electrophilic attacks than DNA from the ultimate carcinogen: aristolactam–nitrenium ion (Figure 1). For the same reason, it would require fewer tissue samples to carry out a protein analysis than that of a DNA analysis. Second, unlike DNA lesions,<sup>27–31</sup> protein adducts are not repaired by repair enzymes and could accumulate during the lifespan of the proteins;<sup>32</sup> therefore, a higher abundance of protein adducts could be accumulated for analysis. Currently, protein adducts are used to biomonitor the exposure to a variety of carcinogens including aromatic amines, aflatoxin, sulfur mustards, among others.<sup>33–38</sup> Lastly, Sidorenko recently demonstrated the *in vitro* and *in vivo* formation of protein adducts of aristolochic acid I (AAI) by coupling polyacrylamide gel with chemiluminescence detection.<sup>39</sup> However, the chemical structures of the adducts are yet to be characterized, which hampered their detection and quantitation by developing a liquid chromatography–tandem mass spectrometric (LC–MS/MS) method of higher selectivity.

As the foundation of the present study, we recently demonstrated that AAI reacts, through the aristolactam–nitrenium ion intermediate, with the thiol group of endogenous aminothiols to form conjugated metabolites, including aristolactam I (ALI)–cysteine (ALI–Cys), ALI–N-acetylcysteine, and ALI–glutathione (ALI–GSH).<sup>40</sup> These occurred presumably via a mechanism resembling that of the AL–DNA adduct formation.<sup>22,41–44</sup> These results shed light on the feasibility that AAI would form protein adducts by reacting with the thiol group of Cys residues and that the resulting protein adducts could serve as biomarkers of AA exposure.

The goals of the present study were twofold. The first was to develop a highly sensitive and selective LC–MS/MS method to rigorously quantitate the elimination products of ALI–

protein adduct ALI. After validation of the accuracy and precision of the method using a synthetic ALI–GSH adduct, the developed method would be applied to quantitate the *in vitro* formation of the ALI–protein adducts in purified human serum albumin. The second goal was to extend the application of the method to study the exposure time- and concentration-dependent formation of ALI–protein adducts in proteins isolated from the kidney (target organ), liver (nontarget organ), and serum of AAI-exposed rats. It is expected that this novel LC–MS/MS-based method will facilitate the use of ALI–protein adducts as biomarkers and dosimeters for human exposure to AAI.

## EXPERIMENTAL SECTION

**Materials.** All chemicals and reagents were of the highest purity available from commercial suppliers and were used as received unless otherwise specified. Aristolochic acid I (AAI) was obtained from Acros (Morris Plains, NJ). Human serum albumin (HSA), protease from *Streptomyces griseus*, L-cysteine (Cys), L-lysine (Lys), L-arginine (Arg), L-histidine (His), L-aspartic acid (Asp), L-glutamic acid (Glu), L-serine (Ser), L-threonine (Thr), L-asparagine (Asn), L-glutamine (Gln), S-methyl-L-cysteine (S-methyl-Cys), reduced glutathione (GSH), zinc dust, glacial acetic acid, sodium hydride (60% dispersion in mineral oil), iodomethane, and tetrahydrofuran (THF) were purchased from Sigma Chemical Co. (St. Louis, MO). HPLC-grade acetonitrile and methanol were purchased from Tedia (Fairfield, OH). THF was further dried by distillation from sodium and benzophenone under nitrogen before use. Deionized water was further purified using a laboratory water purification system (Cascada, PALL; Port Washington, NY) and was used in all experiments.

**Synthesis of Standards.** A reference standard of ALI was synthesized by reducing AAI using zinc dust in acidic medium (Zn/H<sup>+</sup>), as described previously.<sup>15–19,40</sup> N-Methyl-ALI was synthesized by reacting ALI with sodium hydride and iodomethane as described in the Supporting Information, purified by high-performance liquid chromatography (HPLC), and quantitated by HPLC–UV analysis using ALI as the reference standard (Figure S1). Using a similar method, the ALI–GSH and ALI–Cys adducts were synthesized by incubating AAI with the respective aminothiols (Figures S2 and S3), as reported previously.<sup>40</sup>

**Instrumental Analyses.** HPLC purification and quantitation of ALI, N-methyl-ALI, ALI–Cys, and ALI–GSH were performed on an Agilent 1100 series HPLC system with a diode array detector. HPLC–fluorescence (HPLC–FLD) analyses were performed on a Thermo Dionex Ultimate 3000 UHPLC system (Waltham, MA) coupled to a fluorescence detector. High-resolution mass spectrometry (MS) and MS/MS analyses were performed on a Xevo G2 Q-ToF mass spectrometer equipped with a standard electrospray ionization (ESI) interface (Waters Corporation, Milford, MA). Quantitative LC–MS/MS analyses were performed on a Waters Xevo TQ-XS triple quadrupole MS coupled with an Acquity UPLC system (Waters Corporation, Milford, MA). The protein concentration was determined by UV absorbance at 280 nm ( $A_{280\text{ nm}}$ ) using a Jenway UV–visible spectrophotometer (Staffordshire, U.K.).

**In Vitro Incubations with Zinc/H<sup>+</sup>.** AAI was added at a final concentration of 1.5–29.3  $\mu\text{M}$  to 0.5 mg of HSA and 20 mg of preactivated Zn dust in 0.5 mL of potassium phosphate buffer (50 mM, pH 5.8) and incubated at 37 °C for 16 h, as described previously for *in vitro* AL–DNA adducts formation studies.<sup>22</sup> After separation from the Zn dust by centrifugation (20 000 g, 10 min), HSA in the supernatant was precipitated by adding 4 volumes of ice-cold acetone. The HSA pellets were washed thrice using ice-cold acetone before they were redissolved in water and quantitated by UV spectrophotometry at  $A_{280\text{ nm}}$ . Finally, the ALI–HSA was hydrolyzed using the method described below prior to LC–MS/MS analysis.

**Animal Experiments.** Animal experiments were conducted in accordance with the Animal Ordinance established by the Hong Kong Department of Health, and the protocol was approved by The Hong

Kong University of Science and Technology (HKUST) Committee on Research Practice. Male Sprague–Dawley rats (170–200 g) obtained from the HKUST Animal and Plant Care Facility were used for the study. After acclimatizing for a week, rats were dosed with a single oral dose of 10 mg/kg ( $n = 3$ ) or 30 mg/kg ( $n = 3$ ) of AAI dissolved in 1% sodium bicarbonate (w/v) to investigate the concentration-dependent formation of ALI–protein adducts. Rats ( $n = 3$ ) that received the same volume of the dosing vehicle were used as the control. Twenty-four hours after the AAI administration, rats were sacrificed by decapitation, and the kidney, liver, and whole blood were collected for analysis. In another study to investigate the formation and elimination kinetics of the ALI–protein adducts, rats ( $n = 24$ ) that received a single oral dose of 30 mg/kg of AAI were sacrificed on days 1, 2, 3, 8, 14, 21, 28, and 60 postdosing for analysis.

**Protein Sample Preparation.** Kidney and liver proteins of AAI-exposed rats were isolated by ammonium sulfate precipitation after slices of kidney and liver tissues were homogenized using a high-speed tissue-tearor homogenizer, as described previously.<sup>38,45</sup> The whole blood was allowed to sit undisturbed at room temperature for 30 min, followed by centrifugation (4000 g, 10 min, 4 °C) to remove blood clots. Saturated ammonium sulfate solution was added dropwise to the rat serum until ~60% saturation, agitated gently at room temperature for 30 min, and centrifuged (18 000 g, 10 min) to precipitate out the globulins.<sup>46,47</sup> The supernatant, the albumin solution, was desalted, washed, and concentrated by centrifugation (4500 g, 10 min) in a Nanosep 10K centrifugal device. After the protein content was quantified using UV spectrophotometry at  $A_{280 \text{ nm}}$ , the protein samples were further washed by liquid–liquid extraction of 2 volumes of ethyl acetate (EA) and hydrolyzed to release ALI for LC–MS/MS analysis.

The general strategy for quantitation of the ALI–protein adduct involves successive washing of proteins, release of the protein-bound ALI in proteins, extraction of ALI, addition of internal standards, and quantitation by LC–MS/MS. To release the covalently bound ALI from the adduct, 100  $\mu\text{g}$  of protein sample (dissolved in 100  $\mu\text{L}$  of water) was first washed twice by liquid–liquid extraction of 2 volumes of EA and was then incubated at 100 °C in 2.5 M NaOH for 2 h. After cooling to ambient temperature, the hydrolysates were extracted thrice with 600  $\mu\text{L}$  of EA. The organic layers were combined and dried under a nitrogen stream, and the residue was dissolved in 100  $\mu\text{L}$  of 70% aqueous methanol containing 0.16 nM *N*-methyl-ALI internal standard for LC–MS/MS analysis.

**LC–MS/MS Quantitation of ALI in Tissue-Isolated Proteins or Serum Albumin.** The analysis was performed with 10  $\mu\text{L}$  of the 70% aqueous methanol of each of the reconstituted samples. Samples were injected onto an Acquity UPLC BEH C18 column (2.1  $\times$  100 mm i.d., 1.7  $\mu\text{m}$ ; Waters Corporation, Milford, MA) in a Waters Acquity UPLC system eluted at a flow rate of 0.4 mL/min and 40 °C with the following gradient of acetonitrile in 0.2% acetic acid: 0–5 min, 5–100%; 5–8 min, 100%, followed by 3 min of re-equilibration of the column. The UPLC column was coupled to a Waters Xevo TQ-XS triple quadrupole MS with an ESI source operated in positive mode with the following parameters for voltages and source gas: cone gas, 250 L/h; desolvation gas, 850 L/h; collision gas (argon), 0.15 mL/min; nebulizer gas, 7.0 bar; desolvation temperature, 600 °C; capillary voltage, 1.5 kV; and cone voltage, 35 V. The MS was operated in multiple-reaction-monitoring (MRM) mode with the following MRM transitions: ALI:  $m/z$  294  $\rightarrow$  279 (quantitative; collision energy, 22 eV),  $m/z$  294  $\rightarrow$  251 (qualitative; collision energy, 30 eV); *N*-methyl-ALI internal standard:  $m/z$  308  $\rightarrow$  293 (collision energy, 22 eV; Figure S4).

**Calibration and Method Validation.** A matrix-matched calibration curve was used for the quantitative analysis. Working standard solutions were prepared by spiking blank HSA sample matrix with different concentrations of ALI (0.01–0.68 nM) and a fixed concentration of *N*-methyl-ALI (0.16 nM) and analyzed using the LC–MS/MS method stated above. The calibration curve was established by plotting the peak area ratios of ALI to *N*-methyl-ALI versus the concentration of ALI in calibration standards (Figure S5). The limit of detection was estimated as the concentration of ALI that

generates a signal three times the background noise in blank HSA sample matrix.<sup>18</sup>

The efficiency of the hydrolysis and extraction steps was determined using the ALI–GSH adduct, which provides a critical correction for the loss of ALI during sample processing. The validation entailed spiking 100  $\mu\text{g}$  of HSA with 2.2, 22, and 220 fmol of ALI–GSH standard followed by heat and alkaline-catalyzed hydrolysis of the adduct, extraction of ALI from the hydrolysates using EA, and LC–MS/MS analysis of extracts, as described above. The overall efficiency of the method was calculated as the measured quantities of liberated ALI divided by the quantities of added ALI–GSH.

## RESULTS AND DISCUSSION

To the best of our knowledge, the chemical structures of AA–protein adducts had not been reported until recent identification of a series of AAI–aminothiol conjugates.<sup>40</sup> It was proposed that AAI is converted into a reactive aristolactam–nitrenium ion intermediate through enzymatic reduction of its nitro group, which reacts with the nucleophilic thiol group of Cys residues to form covalent carbon–sulfur linkages (Figure 1), similar to that of the AL–DNA adduct formation.<sup>22,41–44</sup>

Because AL–DNA adducts are formed by reacting the aristolactam–nitrenium ion intermediate with the exocyclic amino group of purine nucleotides in DNA, and previous studies identified a broad spectrum of Lys adduct formed by reacting Lys residues with chemical carcinogens such as aflatoxin and formaldehyde,<sup>33,42,45</sup> we further tested the plausible conjugation reaction between the AAI reactive intermediate and Lys residues. Incubation of AAI and Lys in the presence of  $\text{Zn}/\text{H}^+$  yielded no predicted adduct peak in the chromatogram (Figure S3), indicating that the aristolactam–nitrenium ion intermediate is not targeting the amino group of Lys residues. Furthermore, no signal of predicted adduct peaks was detected when Lys was replaced with other amino acids that possess a nucleophilic side chain (Arg, His, Asp, Glu, Ser, Thr, Asn, and Gln).

Based on this foundation and the previous knowledge that serum albumin contains a free Cys residue at position 34 (Cys<sup>34</sup>) that is reactive toward many oxidants and electrophiles,<sup>33,48</sup> we developed and validated a method, using ALI–GSH tripeptide adduct and ALI–HSA, to quantitate ALI–protein adducts in HSA exposed to AAI, tissues, and sera collected from AAI-exposed rats.

**Choice of Hydrolysis Method and Elimination Product.** Prior to the optimization of the hydrolysis conditions for LC–MS/MS analysis, we first compared the performance of enzymatic and chemical hydrolysis using ALI–GSH adduct. ALI–GSH standard was prepared by HPLC purification of the reaction product of a reaction of AAI with GSH, as described in Experimental Section. By spiking 2.2 pmol of ALI–GSH standard into 100  $\mu\text{g}$  of HSA followed by protease digestion as reported previously,<sup>45</sup> it was discovered that the level of ALI–GSH remained stable, and no elimination products were observed by HPLC–FLD analysis (Figure S6).

Attempts were then made to hydrolyze ALI–GSH at 100 °C in 1.0 M HCl/NaOH for 1 h, which are the conditions previously stated by Krumbiegel et al. for hydrolyzing ALI–conjugated metabolites.<sup>49</sup> Results showed heat/ $\text{H}^+$  treatment hydrolyzed ALI–GSH to a complex mixture, including ALI–Cys, two unknown but highly fluorescent products, and ALI as

a minor product (Figure S6). Due to the complexity of the reaction, further acid treatment was not carried out.

We then tested the effect of heat and base (heat/OH<sup>-</sup>) treatment on the release of the ALI–protein adduct for analysis. Results showed that heating ALI–GSH in NaOH solution liberated ALI as the sole product and at a signal intensity sevenfold higher than that with HCl hydrolysis (Figure S6). This observation is in line with our finding that the five-membered lactam ring of ALI is more stable in alkaline than in acid hydrolysis, which will be discussed in a later section (Figure S7). Together with the significantly higher sensitivity (25-fold higher) of ALI over ALI–Cys in LC–MS/MS analysis as reported previously,<sup>40</sup> subsequent study focuses on the use of heat/OH<sup>-</sup> treatment to liberate ALI from ALI-bound proteins for the quantitation of protein adducts by LC–MS/MS analysis.

**Optimization of the Hydrolysis Conditions.** Using ALI–HSA samples obtained from incubating AAI with HSA as described above, we first investigated the number of ethyl acetate (EA) washings required to remove unbound ALI in the proteins. Results showed that the ALI signals in LC–MS/MS analysis of EA extracts from the hydrolysates remained stable after the second washing (Figure S8), suggesting that the unbound ALI produced during *in vitro* incubation of AAI with zinc dust was removed by two times of EA washing. Therefore, in the following experiments, protein samples were washed two times by liquid–liquid extraction of 2 volumes of EA before protein hydrolysis.

After removing the unbound ALI in the protein sample, we optimized the conditions to achieve the highest hydrolysis efficiency on liberating covalently bound ALI from ALI-modified proteins for analysis (Figure 1). By heating the ALI–HSA dissolved in different concentrations of NaOH (0.1–4 M) at 100 °C for 1 h, it was observed that heating in 2.5 M NaOH gave the strongest ALI signal in LC–MS/MS analysis (Figure 2A). Given that the released ALI from ALI–HSA is the most abundant at this condition, we used 2.5 M NaOH as the hydrolysis medium for the cleavage of the covalently bound ALI–protein adducts in subsequent experiments.

We then investigated the effect of the heating temperature on the amount of ALI liberated from the hydrolysis of ALI-bound proteins. By heating the ALI–HSA dissolved in 2.5 M NaOH at different temperatures (22–120 °C) for 1 h, it turned out that 100 °C was the most efficient temperature for hydrolysis (Figure 2B). Further increase in the heating temperature resulted in significant ALI signal loss, probably due to the thermal decomposition of ALI in a highly alkaline environment at elevated temperatures; 100 °C was thus adopted as the hydrolysis temperature in subsequent experiments.

After optimization of the hydrolysis medium and temperature, we evaluated the effect of the incubation time on the yield of ALI in the alkaline hydrolysis of ALI–HSA samples. Our results showed that the amount of ALI liberated from the hydrolysis plateaued within the first 2 h of incubation (Figure 2C). The analytical signal of ALI then declined as incubation progressed, which could be attributed to a more extensive hydrolysis of the lactam ring in ALI at longer incubation times. As a result, protein samples in the entire study were hydrolyzed by heating at 100 °C in 2.5 M NaOH for 2 h before LC–MS/MS analysis.

**Method Validation.** Following optimization of the hydrolysis conditions, we validated the analytical method and

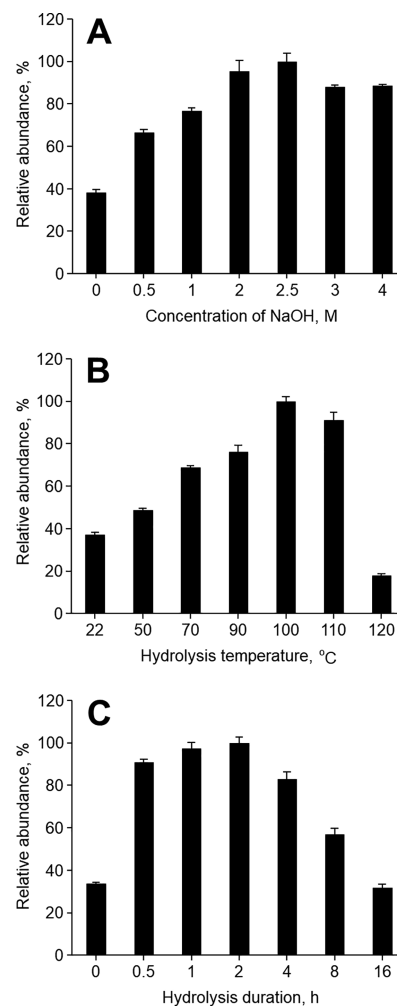


**Figure 2.** Optimization of (A) the concentration of NaOH, (B) the hydrolysis temperature, and (C) the hydrolysis duration on the release of aristolactam I from aristolactam I-bound human serum albumin. Plotted is the relative abundance of aristolactam I from LC–MS/MS analysis of the hydrolysates. The values represent the mean  $\pm$  SD from three independent measurements.

determined the overall efficiency of the hydrolysis and extraction steps using synthetic ALI–GSH adduct. By spiking 100  $\mu$ g of purified HSA with known quantities of the ALI–GSH standard followed by heat/OH<sup>-</sup>-catalyzed release of ALI and LC–MS/MS analysis of EA extracts as described in the Experimental Section, the average yield of ALI was found to be  $66.5 \pm 0.6\%$  of the theoretical values (Table 1), which represents the overall efficiency for the analytical method.

Efforts were also made to identify the causes of the observed deviation from the theoretical values. To this end, 0.17 pmol of purified ALI standard was spiked to 100  $\mu$ g of HSA and was subjected to hydrolysis and EA extraction. Two control groups were prepared by adding the same amount of ALI standard separately to blank HSA hydrolysate followed by EA extraction or EA extracts from blank HSA hydrolysate. All EA extracts were then preconcentrated and analyzed by LC–MS/MS analysis. By comparison of the amount of ALI recovered after hydrolysis with the two control groups, results showed  $\sim 30\%$  of ALI was lost in the alkaline hydrolysis and extraction steps (Figure S7), of which only 5% loss was from the EA extraction process. This loss of ALI ( $\sim 25\%$ ) in the heat/OH<sup>-</sup> treatment process is probably due to the hydrolysis of the amide bond in

**Table 1.** Intraday and Interday Reproducibility and Recovery of the Developed Method for the Analysis of Aristolactam I–Protein Adducts in Human Serum Albumin

	spiked, fmol <sup>a</sup>	accuracy <sup>a</sup>		precision	
		found, fmol	recovery, %	intraday <sup>c,d</sup>	interday <sup>d,e</sup>
ALI–GSH	2.2	1.46 ± 0.08	67.1 ± 3.5	5.2	9.2
	22	14.4 ± 1.0	65.9 ± 4.4	6.7	8.1
	220	144.9 ± 3.2	66.5 ± 1.5	2.2	5.1

<sup>a</sup> $n = 5$ . <sup>b</sup>Amount of ALI–GSH adduct added to 100  $\mu\text{g}$  of HSA. <sup>c</sup>Five replicated analyses in a day. <sup>d</sup>Data presented as % RSD. <sup>e</sup>Analysis performed on five different days of the week.

the lactam ring of ALI into the ring-opened form.<sup>50</sup> The same set of experiments was repeated using 2.5 M HCl, and ~40% of ALI was lost due to acid hydrolysis, which provided another piece of evidence showing the advantage of using alkaline hydrolysis in liberating ALI from ALI-bound proteins. The measurement of ALI was thus corrected by a factor of 1.5 to arrive at the actual quantity of ALI–protein adduct.

Furthermore, we evaluated the precision of the method by analyzing spiked samples on the same day ( $n = 5$ ) and on five different days of the week using the developed LC–MS/MS method. Our method showed excellent reproducibility with percent relative standard deviation smaller than 10 among all the intra- and interday analyses (Table 1), indicating that our method is accurate and precise for the quantitation of the ALI–protein adduct.

The final step of the method validation was to determine the stability of the protein adducts during the protein extraction steps using ALI–HSA samples. As indicated by the similar adduct levels in samples that were treated with and without going through the protein isolation process (Figure S9), these adducts were also found to be stable during protein extraction from both tissue and serum samples, as described in the Experimental Section.

**Quantitation of the ALI–Protein Adducts in Human Serum Albumin Treated with AAI.** The validated method was applied to quantitate ALI hydrolyzed from HSA exposed to AAI activated by  $\text{Zn}/\text{H}^+$ , as described in the Experimental Section. Figure 3 illustrates the concentration-dependent formation of ALI–protein adducts. Linear regression analysis of a plot of the quantities of ALI–HSA adducts versus the concentrations of AAI generates a regression line of  $y = 63.6x - 4.8$  ( $r^2 = 0.999$ ). The exposure produced  $63.6 \pm 1.1$  ALI–HSA adducts per  $10^9$  amino acids per  $\mu\text{M}$  AAI.

**Quantitation of the ALI–Protein Adducts in Internal Organs of AAI-Exposed Rats.** The feasibility of detecting ALI–protein adducts in purified protein was then extended to quantitate the adduct in the protein samples isolated from the kidney (target organ) and liver (nontarget organ) of AAI-exposed rats. Figure 4B shows a typical chromatogram obtained from LC–MS/MS analysis of a kidney protein sample from rats dosed with 30 mg/kg of AAI. The analysis detected a concentration-dependent formation of the adduct in both the kidney and liver (Figure 5) of rats that were dosed with 10 and 30 mg/kg of AAI, with the adduct detected at ~8 and ~30 adducts per  $10^9$  amino acids, respectively. To the best of our knowledge, this is the first report of quantitating ALI–protein adducts in the internal organs of rats. It is worth mentioning that there is no observable difference in the adduct

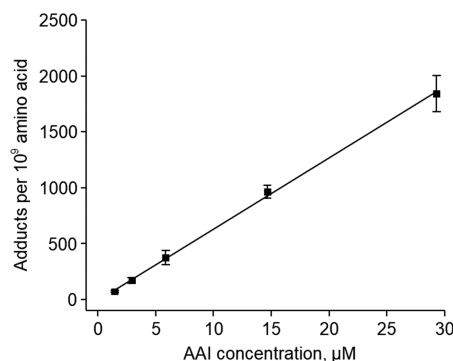


**Figure 3.** Quantitation of aristolactam I in human serum albumin exposed to different concentrations of aristolochic acid I. Human serum albumin was treated with the aristolochic acid I and quantified by LC–MS/MS as described in the Experimental Section. The data represent mean  $\pm$  SD for three independent experiments. Fitting the data by linear regression yielded a line with an equation of  $y = 63.6x - 4.8$  ( $r^2 = 0.999$ ) for human serum albumin.

concentration between kidneys and livers on day 1 postdosing, which is similar to that observed in a previous ALI–DNA adduct study.<sup>41</sup> No ALI was detected in the hydrolysate of protein samples isolated from the internal organs of control rats.

After the identification and quantitation of the ALI–protein adducts in the internal organs of AAI-exposed rats, the study was extended to investigate the stability of the adducts in the liver and kidney for up to 60 days after the oral gavage of AAI to the rats at 30 mg/kg. LC–MS/MS analysis of the tissue-isolated protein samples revealed increasing ALI–protein adduct concentration from day 1 to day 2 of post AAI administration, after which the adduct levels declined but remained quantifiable on day 21 postdosing. The adducts were detectable on day 28 at levels below the method quantitation limit (0.6 adducts per  $10^9$  amino acids); the adduct levels on day 60 postdosing were found below the method detection limit (0.2 adducts per  $10^9$  amino acids). The results of the analysis of the ALI–protein adduct in protein samples isolated from AAI-dosed rats are shown in Figure 5.

The highest adduct level was detected in the renal cortex, which is the tumor-targeting region of the kidney, followed by the renal medulla and liver (Figure 5). Despite the ALI–protein adduct being detected at lower concentrations than that of the ALI–DNA adducts, a similar concentration profile and organotrophic distribution were observed in a previous ALI–DNA adduct study.<sup>41</sup> The results showed a good correlation of ALI–protein adducts with ALI–DNA adducts, suggesting that the formation of protein adducts could also contribute to the observed toxicity of AAs and highlighting the feasibility of using ALI-bound proteins as the target biomacromolecule for assessing exposure to AAI.

The half-lives of the ALI–protein adducts in liver, renal cortex, and renal medulla were estimated as 3.9, 3.2, and 3.3 days, respectively, assuming first-order elimination kinetics. These values are similar to the half-life of rat liver proteins (1.8–3.8 days),<sup>51</sup> suggesting that protein turnover could be a major determinant for the adduct elimination. However, it is believed that the short half-lives for the ALI–protein adduct may not hamper its application as a biomarker for AA exposure. Previous studies reported that residents of rural farming villages in Balkan Peninsula are continuously exposed to AAI through their diets;<sup>15–18</sup> this long-term AAI exposure

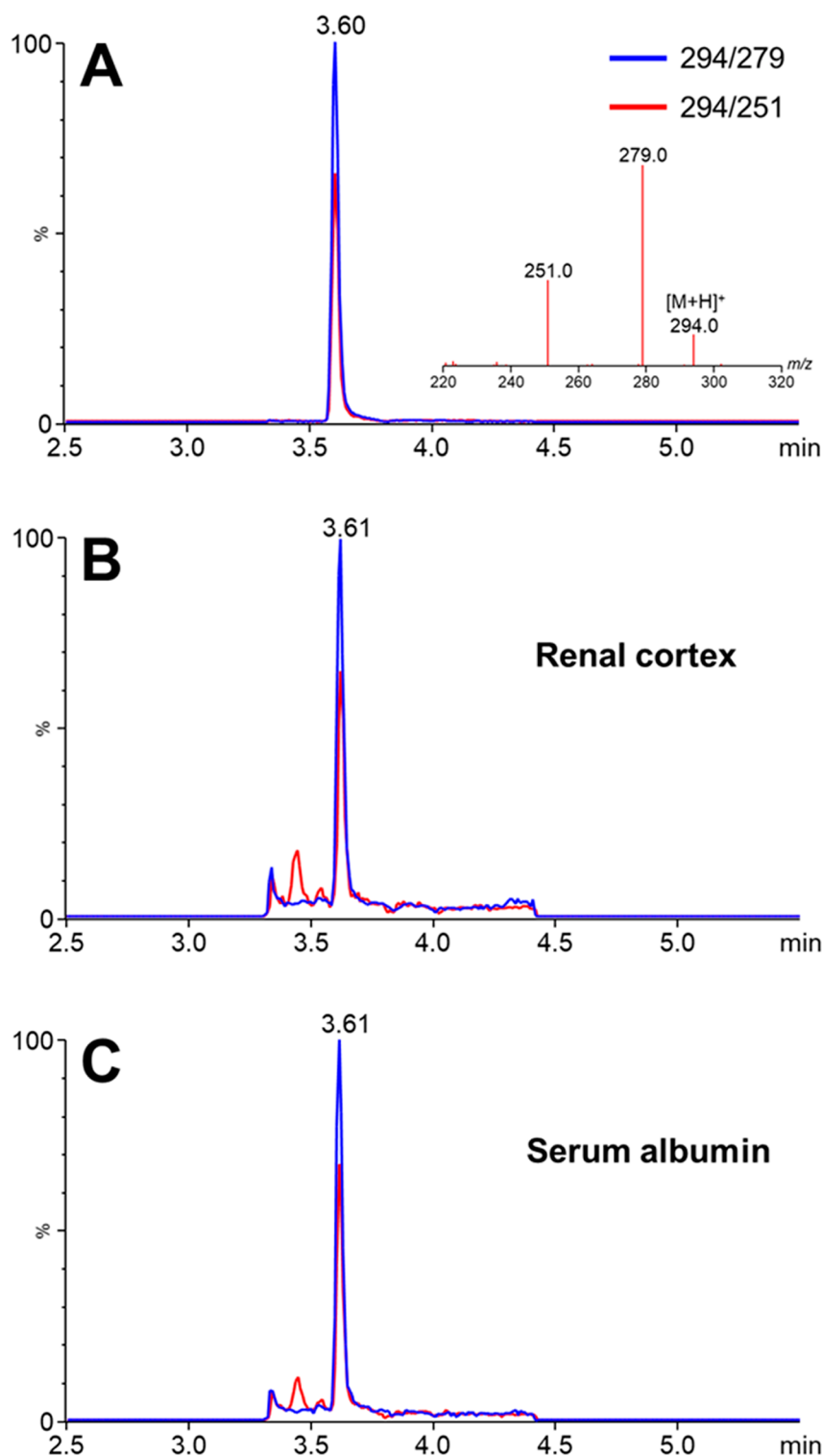


**Figure 4.** Typical chromatograms obtained from LC–MS/MS analysis of aristolactam I in (A) reference standard, (B) the hydrolysates of protein isolated from the renal cortex of aristolochic acid I-exposed rats, and (C) the hydrolysates of albumin isolated from serum of aristolochic acid I-exposed rats.

could provide a continuous supply of AAI, consequently the aristolactam–nitrenium ion intermediate, to react with proteins and maintain a steady level of ALI–protein adducts in human bodies for detection. A long-term and multidose study may be required to reveal the effects of prolonged AAI exposure on the levels of ALI–protein adducts *in vivo*.

**Quantitation of the ALI–Albumin Adducts in the Serum of AAI-Exposed Rats.** Since hepatocyte is the primary site for albumin synthesis and drug metabolism, the reactive electrophiles,<sup>52,53</sup> such as the aristolactam–nitrenium ion in this study, are likely to conjugate with albumin without moving across the cell membrane to reach blood capillaries.<sup>33</sup> This increases the chance of protein adduct formation by

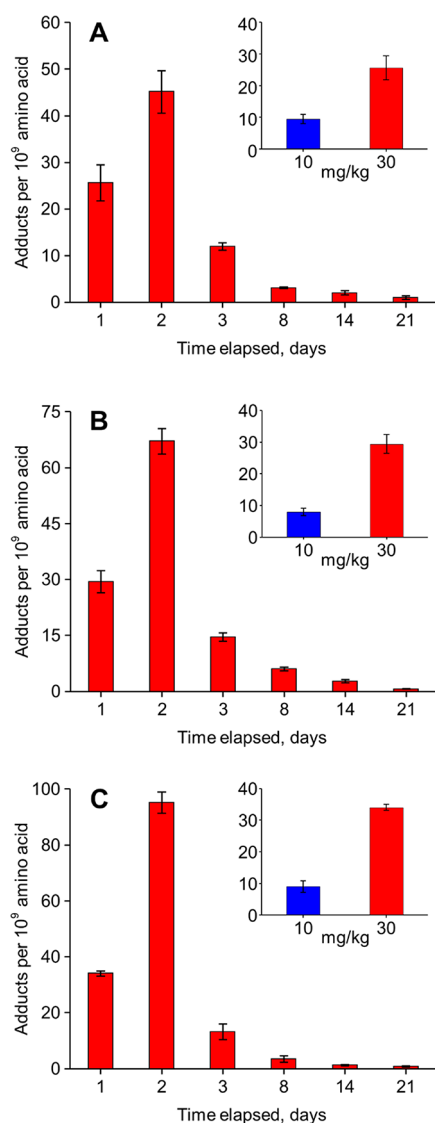


**Figure 5.** Concentrations of aristolactam I–protein adducts in (A) liver, (B) renal medulla, and (C) renal cortex of rats exposed to aristolochic acid I. Rats were exposed to a single oral dose of 30 mg/kg of aristolochic acid I and sacrificed on different days postdosing. Kidney and liver were harvested and aristolactam I–protein adduct in the tissue-isolated protein samples quantified by LC–MS/MS as described in the Experimental Section. The data represent mean  $\pm$  SD for three independent experiments. Insets show the concentration-dependent formation of the adduct in tissue-isolated proteins of rats treated with 10 and 30 mg/kg of aristolochic acid I and sacrificed 24 h after the aristolochic acid I administration. No adduct was detected in the tissue-isolated protein samples of the control rats.

preventing the potential degradation of reactive intermediates during their transport to target organs in the blood vessels,<sup>33</sup> and we therefore further investigate the *in vivo* formation of the ALI–albumin adduct in rat serum.

Figure 4C shows a typical chromatogram obtained from LC–MS/MS analysis of rat serum sample from rats dosed with 30 mg/kg of AAI. Concentration-dependent formation of the ALI–albumin adduct was also observed in the sera of rats that were dosed with 10 and 30 mg/kg of AAI (Figure 6). Specifically, we identified significantly higher levels of the ALI–protein adduct in serum after 24 h of AAI administration, with the highest being detected at  $\sim$ 300 adducts per 10<sup>9</sup> amino

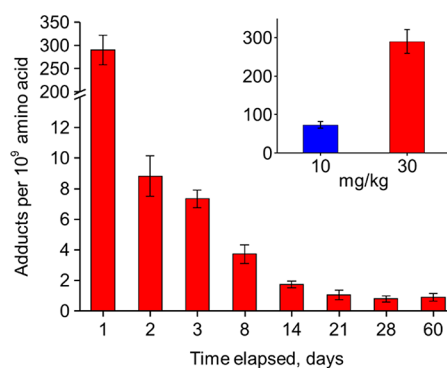


**Figure 6.** Concentrations of aristolactam I–protein adducts in the serum albumin of rats exposed to aristolochic acid I. Rats were exposed to a single oral dose of 30 mg/kg of aristolochic acid I and sacrificed at different days postdosing. Serum albumin was isolated, and the aristolactam I–protein adduct in the samples was quantified by LC–MS/MS as described in the Experimental Section. The data represent mean  $\pm$  SD for three independent experiments. Insets show the concentration-dependent formation of the adduct in rats treated with 10 and 30 mg/kg of aristolochic acid I and sacrificed 24 h after the aristolochic acid I administration. No adduct was detected in the samples of the control rats.

acids. The huge drop in albumin adduct levels from day 1 to day 2 postdosing could be related to the transport function of albumin, as albumin was reported to deliver various substances including drug and ultimate carcinogenic/toxic metabolites around the human bodies.<sup>54,55</sup> This was also supported by the maximum ALI–protein adduct levels detected in tissues on day 2 postdosing (Figure 5).

Furthermore, the adduct remained detectable in the serum even 2 months after a single oral dose of AAI (Figure 6), and the half-life for its first-order decay was calculated to be 4.6 days, which was slightly longer than that of unmodified albumin in normal rats (2.5–3 days) and those of ALI–protein adducts in rat tissues.<sup>56</sup> No ALI was detected in the hydrolysate of serum samples isolated from control rats. These results laid a solid foundation for using the ALI–albumin adduct as a biomarker of AAI exposure in clinical practice.

## CONCLUSIONS

We developed and validated a highly sensitive and selective LC–MS/MS method for the quantitation of the ALI–protein adduct as a biomarker of AA exposure. Results of the studies demonstrated, for the first time, the concentration-dependent formation of ALI–protein adducts in purified serum albumin and in proteins isolated from tissues and sera of AAI-exposed rats. We expect this newly developed method would facilitate the adoption of the ALI–protein adduct as a novel AAI exposure biomarker for conducting molecular epidemiological studies in regions facing AA-induced environmental and food contamination.<sup>15–20,57,58</sup> These works should be beneficial to countries that are conducting traditional herbal medicine practice and to the large number of patients suffering from or at risk of developing CKD due to potential exposures to AAs that are unknown to them.<sup>5,12</sup>

## ASSOCIATED CONTENT

### Supporting Information

The Supporting Information is available free of charge at <https://pubs.acs.org/doi/10.1021/acs.chemrestox.0c00454>.

Experimental section; HPLC and LC–MS spectra; efficiency of hydrolysis; effect of EA washing and stability of ALI–protein adducts (PDF)

## AUTHOR INFORMATION

### Corresponding Authors

**Ning Liu** – Central Laboratory, The Second Hospital of Jilin University, Key Laboratory of Zoonosis Research, Ministry of Education, Jilin University, Changchun, China; [orcid.org/0000-0002-7925-8535](https://orcid.org/0000-0002-7925-8535); Email: [liu\\_ning@jlu.edu.cn](mailto:liu_ning@jlu.edu.cn)

**Wan Chan** – Department of Chemistry, The Hong Kong University of Science and Technology, Kowloon, Hong Kong; [orcid.org/0000-0001-8479-3172](https://orcid.org/0000-0001-8479-3172); Phone: +852 2358-7370; Email: [chanwan@ust.hk](mailto:chanwan@ust.hk); Fax: +852 2358-1594

### Authors

**Chi-Kong Chan** – Department of Chemistry, The Hong Kong University of Science and Technology, Kowloon, Hong Kong; [orcid.org/0000-0001-7963-8725](https://orcid.org/0000-0001-7963-8725)

**Kwan-Kit Jason Chan** – Department of Chemistry, The Hong Kong University of Science and Technology, Kowloon, Hong Kong

Complete contact information is available at:

<https://pubs.acs.org/10.1021/acs.chemrestox.0c00454>

### Author Contributions

C.-K.C., N.L., and W.C. designed the research; C.-K.C. conducted the experiments; C.-K.C., K.-K.J.C., N.L., and W.C. analyzed the data; C.-K.C., N.L., and W.C. wrote the paper.

### Notes

The authors declare no competing financial interest.

## ACKNOWLEDGMENTS

We gratefully acknowledge financial support for this work from the Research Grant Council of Hong Kong (GRF 16303719). C.-K.C. was supported by a Hong Kong Ph.D. Fellowship Scheme from the University Grants Committee of Hong Kong. We also thank Ms. Wendy Lai, Mr. Jack Tung, Ms. Jiayin Zhang, and Mr. Danny Wong for their assistance with sample preparation in this project.

## REFERENCES

- (1) Bikbov, B., Purcell, C. A., Levey, A. S., Smith, M., et al. (2020) Global, Regional, and National Burden of Chronic Kidney Disease, 1990–2017: A Systematic Analysis for the Global Burden of Disease Study 2017. *Lancet* 395, 709–733.
- (2) Zhang, L., Wang, F., Wang, L., Wang, W., Liu, B., Liu, J., Chen, M., He, Q., Liao, Y., Yu, X., Chen, N., Zhang, J., Hu, Z., Liu, F., Hong, D., Ma, L., Liu, H., Zhou, X., Chen, J., Pan, L., Chen, W., Wang, W., Li, X., and Wang, H. (2012) Prevalence of Chronic Kidney Disease in China: A Cross-Sectional Survey. *Lancet* 379, 815–822.
- (3) Couser, W. G., Remuzzi, G., Mendis, S., and Tonelli, M. (2011) The Contribution of Chronic Kidney Disease to the Global Burden of Major Noncommunicable Diseases. *Kidney Int.* 80, 1258–1270.
- (4) Nugent, R. A., Fathima, S. F., Feigl, A. B., and Chyung, D. (2011) The Burden of Chronic Kidney Disease on Developing Nations: A 21st Century Challenge in Global Health. *Nephron. Clin. Pract.* 118, c269–c277.
- (5) Gifford, F. J., Gifford, R. M., Eddleston, M., and Dhaun, N. (2017) Endemic Nephropathy Around the World. *Kidney Int. Rep.* 2, 282–292.
- (6) Jayasumana, C., Orantes, C., Herrera, R., Almaguer, M., Lopez, L., Silva, L. C., Ordunez, P., Siribaddana, S., Gunatilake, S., and De

Broe, M. E. (2016) Chronic Interstitial Nephritis in Agricultural Communities: A Worldwide Epidemic with Social, Occupational and Environmental Determinants. *Nephrol., Dial., Transplant.* 32, 234–241.

(7) Radhakrishnan, J., Remuzzi, G., Saran, R., Williams, D. E., Rios-Burrows, N., Powe, N., Brück, K., Wanner, C., Stel, V. S., Venuthurupalli, S. K., Hoy, W. E., Healy, H. G., Salisbury, A., Fassett, R. G., O'Donoghue, D., Roderick, P., Matsuo, S., Hishida, A., Imai, E., and Imuro, S. (2014) Taming the Chronic Kidney Disease Epidemic: A Global View of Surveillance Efforts. *Kidney Int.* 86, 246–250.

(8) Chan, C.-K., Liu, Y., Pavlović, N. M., and Chan, W. (2019) Aristolochic Acids: Newly Identified Exposure Pathways of this Class of Environmental and Food-Borne Contaminants and its Potential Link to Chronic Kidney Diseases. *Toxics* 7, 14.

(9) Yang, L., Su, T., Li, X.-M., Wang, X., Cai, S.-Q., Meng, L.-Q., Zou, W.-Z., and Wang, H.-Y. (2012) Aristolochic Acid Nephropathy: Variation in Presentation and Prognosis. *Nephrol., Dial., Transplant.* 27, 292–298.

(10) Zhang, J., Zhang, L., Wang, W., and Wang, H. (2013) Association Between Aristolochic Acid and CKD: A Cross-Sectional Survey in China. *Am. J. Kidney Dis.* 61, 918–922.

(11) Jelaković, B., Castells, X., Tomić, K., Ardin, M., Karanović, S., and Zavadil, J. (2015) Renal Cell Carcinomas of Chronic Kidney Disease Patients Harbor the Mutational Signature of Carcinogenic Aristolochic Acid. *Int. J. Cancer* 136, 2967–2972.

(12) Li, W., Hu, Q., and Chan, W. (2016) Uptake and Accumulation of Nephrotoxic and Carcinogenic Aristolochic Acids in Food Crops Grown in *Aristolochia Clematitis*-Contaminated Soil and Water. *J. Agric. Food Chem.* 64, 107–112.

(13) Grollman, A. P. (2013) Aristolochic Acid Nephropathy: Harbinger of a Global Iatrogenic Disease. *Environ. Mol. Mutagen.* 54, 1–7.

(14) Grollman, A. P., Shibutani, S., Moriya, M., Miller, F., Wu, L., Moll, U., Suzuki, N., Fernandes, A., Rosenquist, T., Medverec, Z., Jakovina, K., Brdar, B., Slade, N., Turesky, R. J., Goodenough, A. K., Rieger, R., Vukelić, M., and Jelaković, B. (2007) Aristolochic Acid and the Etiology of Endemic (Balkan) Nephropathy. *Proc. Natl. Acad. Sci. U. S. A.* 104, 12129–12134.

(15) Chan, W., Pavlović, N. M., Li, W., Chan, C.-K., Liu, J., Deng, K., Wang, Y., Milosavljević, B., and Kostić, E. N. (2016) Quantitation of Aristolochic Acids in Corn, Wheat Grain, and Soil Samples Collected in Serbia: Identifying a Novel Exposure Pathway in the Etiology of Balkan Endemic Nephropathy. *J. Agric. Food Chem.* 64, 5928–5934.

(16) Li, W., Chan, C.-K., Liu, Y., Yao, J., Mitić, B., Kostić, E. N., Milosavljević, B., Davinić, I., Orem, W. H., Tatu, C. A., Dedon, P. C., Pavlović, N. M., and Chan, W. (2018) Aristolochic Acids as Persistent Soil Pollutants: Determination of Risk for Human Exposure and Nephropathy From Plant Uptake. *J. Agric. Food Chem.* 66, 11468–11476.

(17) Chan, C.-K., Pavlović, N. M., and Chan, W. (2019) Development of a Novel Liquid Chromatography–Tandem Mass Spectrometric Method for Aristolochic Acids Detection: Application in Food and Agricultural Soil Analyses. *Food Chem.* 289, 673–679.

(18) Tung, K.-K., Chan, C.-K., Zhao, Y., Chan, K.-K. J., Liu, G., Pavlović, N. M., and Chan, W. (2020) Occurrence and Environmental Stability of Aristolochic Acids in Groundwater Collected From Serbia: Links to Human Exposure and Balkan Endemic Nephropathy. *Environ. Sci. Technol.* 54, 1554–1561.

(19) Chan, C.-K., Chan, K.K. J., Pavlović, N. M., and Chan, W. (2020) Liquid Chromatography–Tandem Mass Spectrometry Analysis of Aristolochic Acids in Soil Samples Collected from Serbia: Link to Balkan Endemic Nephropathy. *Rapid Commun. Mass Spectrom.* 34, e8547.

(20) Chan, C.-K., Tung, K.-K., Pavlović, N. M., and Chan, W. (2020) Remediation of Aristolochic Acid-Contaminated Soil by an Effective Advanced Oxidation Process. *Sci. Total Environ.* 720, 137528.

- (21) Jelaković, B., Karanović, S., Vuković-Lela, I., Miller, F., Edwards, K. L., Nikolić, J., Tomić, K., Slade, N., Brdar, B., Turesky, R. J., Stipančić, Ž., Dittrich, D., Grollman, A. P., and Dickman, K. G. (2012) Aristolactam-DNA Adducts are a Biomarker of Environmental Exposure to Aristolochic Acid. *Kidney Int.* 81, 559–567.
- (22) Yun, B. H., Rosenquist, T. A., Sidorenko, V., Iden, C. R., Chen, C.-H., Pu, Y.-S., Bonala, R., Johnson, F., Dickman, K. G., Grollman, A. P., and Turesky, R. J. (2012) Biomonitoring of Aristolactam-DNA Adducts in Human Tissues Using Ultra-Performance Liquid Chromatography/Ion-Trap Mass Spectrometry. *Chem. Res. Toxicol.* 25, 1119–1131.
- (23) Turesky, R. J., Yun, B. H., Brennan, P., Mates, D., Jinga, V., Harnden, P., Banks, R. E., Blanche, H., Bihoreau, M.-T., Chopard, P., Letourneau, L., Lathrop, G. M., and Scelo, G. (2016) Aristolochic Acid Exposure in Romania and Implications for Renal Cell Carcinoma. *Br. J. Cancer* 114, 76–80.
- (24) Hogan, J. J., Mocanu, M., and Berns, J. S. (2016) The Native Kidney Biopsy: Update and Evidence for Best Practice. *Clin. J. Am. Soc. Nephrol.* 11, 354–362.
- (25) Williams, W. W., Taheri, D., Tolckoff-Rubin, N., and Colvin, R. B. (2012) Clinical Role of the Renal Transplant Biopsy. *Nat. Rev. Nephrol.* 8, 110–121.
- (26) Chandrashekar, K. N., and Yakkaladevi, A. (2015) *Basic Concepts in Biotechnology*, 1st ed., Laxmi, Solapur, India.
- (27) Lai, Y., Lu, M., Gao, X., Wu, H., and Cai, Z. (2011) New Evidence for Toxicity of Polybrominated Diphenyl Ethers: DNA Adduct Formation from Quinone Metabolites. *Environ. Sci. Technol.* 45, 10720–10727.
- (28) Chan, S. W., and Dedon, P. C. (2010) The Biological and Metabolic Fate of DNA Damage Products. *J. Nucleic Acids* 2010, 929047.
- (29) Li, J., Leung, E. M. K., Choi, M. M. F., and Chan, W. (2013) Combination of Pentafluorophenylhydrazine Derivatization and Isotope Dilution LC-MS/MS Techniques for the Quantification of Apurinic/Apyrimidinic Sites in Cellular DNA. *Anal. Bioanal. Chem.* 405, 4059–4066.
- (30) Leung, E. M. K., and Chan, W. (2015) Comparison of DNA and RNA Adduct Formation: Significantly Higher Levels of RNA Than DNA Modifications in the Internal Organs of Aristolochic Acid-Dosed Rats. *Chem. Res. Toxicol.* 28, 248–255.
- (31) Leung, E. M. K., and Chan, W. (2014) Noninvasive Measurement of Aristolochic acid-DNA Adducts in Urine Samples from Aristolochic Acid-Treated Rats by Liquid Chromatography Coupled Tandem Mass Spectrometry: Evidence for DNA Repair by Nucleotide-Excision Repair Mechanisms. *Mutat. Res., Fundam. Mol. Mech. Mutagen.* 766–767, 1–6.
- (32) Vineis, P., and Perera, F. (2000) DNA Adducts as Markers of Exposure to Carcinogens and Risk of Cancer. *Int. J. Cancer* 88, 325–328.
- (33) Sabbioni, G., and Turesky, R. J. (2017) Biomonitoring Human Albumin Adducts: The Past, the Present, and the Future. *Chem. Res. Toxicol.* 30, 332–366.
- (34) Dingley, K. H., Curtis, K. D., Nowell, S., Felton, J. S., Lang, N. P., and Turteltaub, K. W. (1999) DNA and Protein Adduct Formation in the Colon and Blood of Humans after Exposure to a Dietary-Relevant Dose of 2-Amino-1-methyl-6-phenylimidazo[4,5-*b*]pyridine. *Cancer Epidemiol. Biomarkers Prev.* 8, 507–512.
- (35) Sabbioni, G., Ambs, S., Wogan, G. N., and Groopman, J. D. (1990) The Aflatoxin-Lysine Adduct Quantified by High-Performance Liquid Chromatography from Human Serum Albumin Samples. *Carcinogenesis* 11, 2063–2066.
- (36) Noort, D., Hulst, A. G., de Jong, L. P. A., and Benschop, H. P. (1999) Alkylation of Human Serum Albumin by Sulfur Mustard in Vitro and in Vivo: Mass Spectrometric Analysis of a Cysteine Adduct as a Sensitive Biomarker of Exposure. *Chem. Res. Toxicol.* 12, 715–721.
- (37) Wang, Y., Villalta, P. W., Peng, L., Dingley, K., Malfatti, M. A., Turteltaub, K. W., and Turesky, R. J. (2017) Mass Spectrometric Characterization of an Acid-Labile Adduct Formed with 2-Amino-1-methyl-6-phenylimidazo[4,5-*b*]pyridine and Albumin in Humans. *Chem. Res. Toxicol.* 30, 705–714.
- (38) Chan, W., Wong, S.-K., and Li, W. (2018) Quantification of DNA and Protein Adducts of 1-Nitropyrene: Significantly Higher Levels of Protein than DNA Adducts in the Internal Organs of 1-Nitropyrene Exposed Rats. *Chem. Res. Toxicol.* 31, 680–687.
- (39) Sidorenko, V. S. (2020) In *Mechanisms of Genome Protection and Repair* (Zharkov, D., Ed.) pp 139–166, Springer, Cham.
- (40) Zhang, J., Chan, C.-K., Ham, Y.-H., and Chan, W. (2020) Identifying Cysteine, N-Acetylcysteine, and Glutathione Conjugates as Novel Metabolites of Aristolochic Acid I: Emergence of a New Detoxification Pathway. *Chem. Res. Toxicol.* 33, 1374–1381.
- (41) Liu, Y., Chan, C.-K., Jin, L., Wong, S.-K., and Chan, W. (2019) Quantitation of DNA Adducts in Target and Nontarget Organs of Aristolochic Acid I-Exposed Rats: Correlating DNA Adduct Levels with Organotropic Activities. *Chem. Res. Toxicol.* 32, 397–399.
- (42) Pfau, W., Schmeiser, H. H., and Wiessler, M. (1990) Aristolochic Acid Binds Covalently to the Exocyclic Amino Group of Purine Nucleotides in DNA. *Carcinogenesis* 11, 313–319.
- (43) Attaluri, S., Bonala, R. R., Yang, I.-Y., Lukin, M. A., Wen, Y., Grollman, A. P., Moriya, M., Iden, C. R., and Johnson, F. (2010) DNA Adducts of Aristolochic Acid II: Total Synthesis and Site-Specific Mutagenesis Studies in Mammalian Cells. *Nucleic Acids Res.* 38, 339–352.
- (44) Stiborová, M., Frei, E., Hodek, P., Wiessler, M., and Schmeiser, H. H. (2005) Human Hepatic and Renal Microsomes, Cytochromes P450 1A1/2, NADPH:Cytochrome P450 Reductase and Prostaglandin H Synthase Mediate the Formation of Aristolochic Acid-DNA Adducts Found in Patients with Urothelial Cancer. *Int. J. Cancer* 113, 189–197.
- (45) Zhao, Y., Chan, C.-K., Chan, K. K. J., and Chan, W. (2019) Quantitation of N<sup>6</sup>-Formyl-lysine Adduct Following Aristolochic Acid Exposure in Cells and Rat Tissues by Liquid Chromatography-Tandem Mass Spectrometry Coupled with Stable Isotope-Dilution Method. *Chem. Res. Toxicol.* 32, 2086–2094.
- (46) Rappaport, S. M., Ting, D., Jin, Z., Yeowell-O'Connell, K., Waidyanatha, S., and McDonald, T. (1993) Application of Raney Nickel to Measure Adducts of Styrene Oxide with Hemoglobin and Albumin. *Chem. Res. Toxicol.* 6, 238–244.
- (47) Wild, C. P., Jiang, Y. Z., Sabbioni, G., Chapot, B., and Montesano, R. (1990) Evaluation of Methods for Quantitation of Aflatoxin-Albumin Adducts and Their Application to Human Exposure Assessment. *Cancer Res.* 50, 245–251.
- (48) Rappaport, S. M., Li, H., Grigoryan, H., Funk, W. E., and Williams, E. R. (2012) Adductomics: Characterizing Exposures to Reactive Electrophiles. *Toxicol. Lett.* 213, 83–90.
- (49) Krumbiegel, G., Hallensleben, J., Mennicke, W. H., Rittmann, N., and Roth, H. J. (1987) Studies on the Metabolism of Aristolochic Acids I and II. *Xenobiotica* 17, 981–991.
- (50) Dubey, R. C. (2014) *A Textbook of Biotechnology*, 5th ed., S. Chand, Ramnagar, India.
- (51) Swick, W. S. (1958) Measurement of Protein Turnover in Rat Liver. *J. Biol. Chem.* 231, 751–764.
- (52) Peters, T. (1985) Serum Albumin. *Adv. Protein Chem.* 37, 161–245.
- (53) Guillouzo, A., Morel, F., Langouët, S., Maheo, K., and Rissel, M. (1997) Use of Hepatocyte Cultures for the Study of Hepatotoxic Compounds. *J. Hepatol.* 26, 73–80.
- (54) Skipper, P. L. (1996) Influence of Tertiary Structure on Nucleophilic Substitution Reactions of Proteins. *Chem. Res. Toxicol.* 9, 918–923.
- (55) Shen, Y., Zhu, C., Wang, Y., Xu, J., Xue, R., Ji, F., Wu, Y., Wu, Z., Zhang, W., Zheng, Z., and Ye, Y. (2020) Evaluation of the Binding of Chelerythrine, a Potentially Harmful Toxin, with Bovine Serum Albumin. *Food Chem. Toxicol.* 135, 110933.
- (56) Sabbioni, G., Skipper, P. L., Büchi, G., and Tannenbaum, S. R. (1987) Isolation and Characterization of the Major Serum Albumin Adduct Formed by Aflatoxin B<sub>1</sub> In Vivo in Rats. *Carcinogenesis* 8, 819–824.

(57) Gruia, A. T., Oprean, C., Ivan, A., Cean, A., Cristea, M., Draghia, L., Damiescu, R., Pavlovic, N. M., Paunescu, V., and Tatu, C. A. (2018) Balkan Endemic Nephropathy and Aristolochic Acid I: An Investigation into the Role of Soil and Soil Organic Matter Contamination, as a Potential Natural Exposure Pathway. *Environ. Geochem. Health* 40, 1437–1448.

(58) Chan, C.-K., Liu, Y., Pavlović, N. M., and Chan, W. (2018) Etiology of Balkan Endemic Nephropathy: An Update on Aristolochic Acids Exposure Mechanisms. *Chem. Res. Toxicol.* 31, 1109–1110.